First Detection of Millimeter/Submillimeter Extragalactic H_2O Maser Emission

E. M. L. Humphreys

ehumphreys@cfa.harvard.edu

L. J. Greenhill

lgreenhill@cfa.harvard.edu

M. J. Reid

mreid@cfa.harvard.edu

H. Beuther

hbeuther@cfa.harvard.edu

J. M. Moran

jmoran@cfa.harvard.edu

M. Gurwell

mgurwell@cfa.harvard.edu

D. J. Wilner

dwilner@cfa.harvard.edu

P. T. Kondratko

pkondratko@cfa.harvard.edu

Harvard-Smithsonian Center for Astrophysics, 60 Garden Street, Cambridge, MA 02138

ABSTRACT

We report the first detection of an extragalactic millimeter wavelength H_2O maser at 183 GHz towards NGC 3079 using the Submillimeter Array (SMA), and a tentative submillimeter wave detection of the 439 GHz maser towards the same source using the James Clerk Maxwell Telescope (JCMT). These H_2O transitions

are known to exhibit maser emission in star-forming regions and evolved stars. NGC 3079 is a well-studied nuclear H_2O maser source at 22 GHz with a time-variable peak flux density in the range 3 – 12 Jy. The 183 GHz H_2O maser emission, with peak flux density $\sim$0.5 Jy (7σ detection), also originates from the nuclear region of NGC 3079 and is spatially coincident with the dust continuum peak at 193 GHz (53 mJy integrated). Peak emission at both 183 and 439 GHz occurs in the same range of velocity as that covered by the 22 GHz spectrum. We estimate the gas to dust ratio of the nucleus of NGC 3079 to be $\approx$150, comparable to the Galactic value of 160. Discovery of maser emission in an active galactic nucleus beyond the long-known 22 GHz transition opens the possibility of future position-resolved radiative transfer modeling of accretion disks and outflows < 1 pc from massive black holes.

Subject headings: Masers — submillimeter — galaxies: active — galaxies: nuclei — galaxies: individual (NGC 3079) — techniques: high angular resolution

1. Introduction

Active galactic nuclei (AGN) that exhibit H_2O maser emission at 22 GHz have been objects of particular interest since discovery that the maser emission can trace circumnuclear accretion disks, as in NGC 4258 (Miyoshi et al. 1995; Greenhill et al. 1995a,b). The presence of maser emission enables direct mapping of AGN dynamics within 1 pc of supermassive black holes via Very Long Baseline Interferometry (VLBI) (see reviews of Greenhill 2002; Maloney 2002). The additional discovery that H_2O maser emission can be associated with shocked gas in jets and outflows has also provided a tracer for a second component in AGN (Gallimore et al. 1996; Claussen et al. 1998; Peck et al. 2003; Greenhill et al. 2003).

Maser emission at 22 GHz is believed to be predominantly collisionally-pumped at gas kinetic temperatures of $T_k = 400$ – 1000 K, hydrogen densities of $n(H_2) = 10^8$ – 10^{10} cm^{-3}, and dust temperatures $T_d < 100$ K (e.g., Deguchi 1977; Elitzur et al. 1989; Yates et al. 1997). In AGN accretion disks, gas heating is thought to arise from X-ray irradiation of the disk surfaces, whereas masers in jets and outflows may be heated via shock compressions (Neufeld et al. 1994; Kartje et al. 1999).

Since the physical conditions that give rise to emission at 22 GHz also pump other H_2O maser transitions, notably those at 183, 321 and 325 GHz (e.g., Deguchi 1977; Neufeld & Melnick 1991; Yates et al. 1997), 22 GHz maser emission is unlikely to be alone in AGN disks, jets and outflows. We note that, in galactic regions of star formation and evolved

stars, inversion of the 22 GHz transition is accompanied by inversion of other rotational transitions from the ground and vibrationally excited H_2O states (e.g., Phillips et al. 1980; Waters et al. 1980; Menten & Melnick 1989; Menten et al. 1990a,b; Feldman et al. 1991; Menten & Melnick 1991; Melnick et al. 1993). In AGN, some of the masers should occur in broadly the same regions as at 22 GHz, but others could probe uncharted regions of the central engines of AGN, including regions at smaller radii. Line ratios of two or more maser transitions originating from the same gas would constrain radiative transfer models far better than is now possible. Previous searches for extragalactic millimeter/submillimeter H_2O masers have been performed, but have been hampered by r.m.s. sensitivities worse than 1 Jy (Menten, private communication).

NGC 3079 is an almost edge-on spiral Seyfert 2/LINER galaxy with optical heliocentric velocity of 1125 ± 6 km s^{-1} (e.g., Heckman 1980; Ho et al. 1997), at a distance of 16 Mpc (Sofue 1999). It hosts 22 GHz H_2O maser emission at velocities between ∼940 and 1350 km s^{-1}, which are believed to trace a disk-like structure at radii of 0.4 – 1.3 pc from a 2×10^6 $M_\odot$ central engine. The pc-scale maser disk is aligned with a dense molecular kpc-scale disk (Koda et al. 2002) and is located at the apex of a kpc-scale superbubble (Kondratko et al. 2005; Cecil et al. 2002). The bubble is believed to be inflated by a wide-angle outflow (Cecil et al. 2001) that is also responsible for the radio continuum lobes along the minor axis of the galaxy (e.g., Duric & Seaquist 1988; Trotter et al. 1998; Sawada-Satoh et al. 2000; Yamauchi et al. 2004). Within a parsec of the nucleus, the relativistic jet appears aligned with the inner wall of the bubble and may be responsible for weak 22 GHz maser emission away from the disk (Kondratko et al. 2005, and references therein). All of these emission sources lie within the primary beam of the SMA observations reported here.

2. Observations and Data Reduction

2.1. SMA Observations at 183 GHz

We observed the ground-state $3_{13} \rightarrow 2_{20}$ transition of para-H_2O (E_u/k ∼200 K) at a rest frequency of 183.310 GHz (λ: 1.6 mm) towards NGC 3079 using the SMA[1] on 2005 March 1. The compact configuration included six antennas, resulting in projected baselines of 8 – 72 m. The SMA receivers operate in double-sideband mode with two 2 GHz sidebands that we tuned to 183.310 and 193.310 GHz (band-center). The correlator provided continuous

[1]The SMA is a joint project between the Smithsonian Astrophysical Observatory and the Academia Sinica Institute of Astronomy and Astrophysics, and is funded by the Smithsonian Institution and the Academia Sinica.

coverage of each sideband (in 24 separate chunks of 256 channels) and 0.4 MHz channel spacing. The phase center of the observations was $\alpha_{2000} = 10^h01^m58^s.53$, $\delta_{2000} = 55^o40'50''.1$ (Cotton et al. 1999). The zenith opacity measured with the NRAO tipping radiometer located at the Caltech Submillimeter Observatory was τ(225 GHz)=0.03 - 0.05 throughout.

We calibrated the data within the IDL superset MIR developed for the Owens Valley Radio Observatory (Scoville 1993) and adapted for the SMA; the imaging was performed in MIRIAD. Data reduction took into account the effect of the pressure-broadened terrestrial H_2O absorption line centered at 183.310 GHz. Fortunately, the redshift of the galaxy reduces the line frequency of the maser transition by ∼0.7 GHz, greatly lowering the corresponding atmospheric opacity. For bandpass calibration we used Jupiter and Saturn. Phase calibration was performed via frequent observations of the quasar 0923+392 about 18° from the phase center. We performed the amplitude calibration separately for upper and lower sideband data. For the upper sideband, we used 0923+392; for lower sideband data, we performed amplitude calibration on each of the 24 spectral chunks separately using Saturn and Jupiter. The calibration of the lower sideband both as a function of elevation and frequency was designed to reduce the effect of variation in terrestrial H_2O absorption across the sideband. We derived the flux scale using observations of Callisto with an estimated accuracy of 20%. Single sideband system temperatures corrected to the top of the atmosphere were between 400 and 850 K.

2.2. JCMT Observations at 439 GHz

We observed the ground-state $6_{43} \rightarrow 5_{50}$ transition of ortho-H_2O (E_u/k ∼1100 K) at a rest frequency of 439.151 GHz (λ: 0.7 mm) towards NGC 3079 using the 15 meter JCMT on 2004 November 18 in τ_{225}=0.041 – 0.045 weather. The instantaneous bandwidth was 1840 MHz, corresponding to ∼1200 km s^{-1}, with a channel spacing of 1250 kHz or 0.85 km s^{-1}. The integration time on source was 2 hrs in beam-switching mode with a throw of 60″. The average T_{sys} during the observations was 2650 K. We reduced the data using the Starlink spectral-line reduction software, SpecX.

3. Results

We detected millimeter (193 GHz) continuum emission with a peak signal to noise ratio (S/N) of ∼10 (Fig. 1) at $\alpha_{2000} = 10^h01^m57^s.80 \pm 0.02$, $\delta_{2000} = 55^o40'46''.9 \pm 0.3$ (statistical uncertainties). Systematic uncertainties of ($0^s.02$,$0''.3$) were estimated through measurement

of an apparent position for 1150+497 against the phase calibrator 0923+392. These place the peak of the millimeter continuum within 1σ of the 22 GHz maser position. We partially resolved the nucleus in the north-south direction and the elongation is approximately parallel to the position angles of both the pc-scale accretion disk traced by 22 GHz maser emission and the kpc-scale molecular disk detected using e.g., CO (Koda et al. 2002).

We detected 183 GHz H_2O emission with a peak S/N of $\sim$7 in both the real part of the amplitude spectrum and the interferometer phase spectrum (Figs. 1 and 2). The peak flux density is 0.55 Jy at 1017 km s^{-1}. The line covers 9 frequency channels and overlaps a persistent Doppler component appearing in published 22 GHz maser spectra for dates 1998 May 8, 2000 March 18 where it is especially prominent at $\sim$2.5 Jy (both Hagiwara et al. 2002), 2001 March 23 (Kondratko et al. 2005) and 2002 April 12 (Braatz et al. 2003). We note possible detection of additional spectral features at 1208 (5 channels wide) and 1265 km s^{-1} (4 channels wide). Both features appear in spectra of real amplitude and phase (near zero degrees, which indicates positions similar to the 1017 km s^{-1} emission), and both lie within the velocity interval of 22 GHz emission. Note that the correspondence of features between 22 and 183 GHz observations is not precise and is also not expected to be true for all features under certain pumping scenarios. The peak maser emission is at $\alpha_{2000} = 10^h01^m57^s.75 \pm 0.03$, $\delta_{2000} = 55^o40'46\farcs7 \pm 0.4$, which is within 1σ of the 193 GHz continuum peak. At our resolution, we cannot determine whether 183 GHz emission originates from the disk or outflow, or from both. We note that in addition to tracing a disk, a subset of 22 GHz maser emission is associated with the outflow within a few parsecs of the nucleus (Kondratko et al. 2005). 22 GHz emission at around 1000 and 1200 km s^{-1} is present both in the disk and outflow. Possible angular extension of the 183 GHz emission to the southeast is marginally detected (2σ), which lies along the axis of the relativistic flow (e.g., Kondratko et al. 2005). We note that Hagiwara et al. (2004) detect OH absorption associated with the outflow at an overlapping velocity, and that we cannot rule out shocks in circumnuclear material as an origin for 183 GHz emission.

We obtained a tentative detection (5σ) of the 439 GHz maser at 1157 km s^{-1} (Fig. 3). With peak S_ν $\sim$2.5 Jy, 439 GHz emission is of comparable strength to typical values for peak 22 GHz emission towards NGC 3079 and occurs within the 22 GHz velocity interval.

4. Discussion

4.1. Millimeter Dust Emission

The millimeter continuum of NGC 3079 is probably dominated by thermal emission from optically thin dust. As in the 1.2 mm observations of Braine et al. (1997) at 11″ resolution, we find dust concentrated in the nuclear region of NGC 3079 (Fig. 1) and place an upper limit of 8 mJy (3σ) on emission associated with the radio lobes ∼1 kpc from the emission peak. Braine et al. (1997) estimates the dust temperature to be ∼30 K at kpc radii. However, in two other AGN the presence of hotter dust at 100 times smaller radii, of ∼300 K, has been inferred from VLT observations (Jaffe et al. 2004; Prieto et al. 2004). Adopting a dust temperature of 100 K for NGC 3079 on intermediate scales and a dust opacity index $\beta = 2$, we estimate the enclosed dust mass of the inner 200 pc is $M_{dust} \sim 10^{6.3\pm0.8}$ $M_\odot$ using the method described in Hildebrand (1983). Using CO Nobeyama observations by Koda et al. (2002), who find a gas mass of M_{gas} $\sim 10^{8.5}$ $M_\odot$ within the central 150 pc, we estimate a gas-to-dust ratio of 150, which is comparable to the Galactic value of 160 and to the ratios derived in bright local galaxies (Dunne et al. 2000).

4.2. 183 GHz Emission

The 183 GHz emission we detect in the nucleus of NGC 3079 is likely from a maser process. It arises from one, and possibly more, narrow unresolved features in the same range of velocity as that of known 22 GHz maser emission. From radiative transfer models we know that the same high densities and temperature conditions that produce maser emission at 22 GHz also strongly invert the 183 GHz H_2O transition. Noting that the 22 GHz feature at 1017 km s^{-1} varies between 0.4 – 2.6 Jy (Hagiwara et al. 2002), and assuming an ortho:para H_2O ratio of 3:1, pumping models could reproduce likely line ratios (e.g., Yates et al. 1997). Narrow linewidths (<8 km s^{-1}) at 183 GHz, small compared with the characteristic rotational and apparent random velocities for molecular gas in this nucleus (Kondratko et al. 2005), also indicate that emitting regions should be compact. Our beam size is too large to determine whether emission is thermal or maser based on brightness temperature arguments. For the emission to be thermal, with a brightness temperature of $\leq$ 2000 K such that H_2O molecules are not dissociated, the emitting region must be $> 0\farcs1$ (10 pc).

4.3. 439 GHz Emission

439 GHz emission is probably also due to maser amplification. Emission occurs over a narrow velocity range (Fig. 3), and conditions for strong 439 GHz inversion are likely to exist in the galactic nucleus. The 22 GHz spectrum peaks to the blue of the v_{sys} of 1125 km s^{-1}, yet the 439 GHz spectrum peaks slightly above v_{sys} at 1157 km s^{-1} (Fig. 3). We ascribe this difference to the different pump mechanisms operating for each maser. Whereas 22 GHz emission is collisionally-pumped and is increasingly quenched by local dust temperatures >100 K, the 439 GHz maser is predominantly radiatively-pumped and is most strongly inverted in the presence of $T_d = 300\ K$, $T_k = 400\ K$ and n(H_2) = 5 x 10^9 cm^{-3} (Yates et al. 1997). Dust temperatures of this order and higher are reasonable in the central parsecs of the nucleus (Jaffe et al. 2004; Prieto et al. 2004). Peak 439 GHz emission (1157 km s^{-1}) is therefore likely to originate from a hot, dusty region around the central engine, possibly at radii $\ll$1 pc, separated spatially from the gas emitting most strongly at 22 GHz (956 km s^{-1}). At 22 GHz, features at these velocities are indeed separated spatially by $\sim$1 pc projected (Kondratko et al. 2005). The observations in Fig. 3 were taken on different dates, and we note that the 22 GHz feature near 1157 km s^{-1} is not present at all epochs (e.g., in Fig. 2). However, the feature line ratio in Fig. 3 of $\sim$100 is accommodated by the vicinity of hot dust (Yates et al. 1997).

We thank the all the SMA and JCMT staff. We thank S. Paine for opacity data, J. Braatz for 22 GHz data and G. Melnick for useful discussions. H. B. acknowledges support from the Emmy-Noether Program of the Deutsche Forschungsgemeinschaft (DFG-BE2578/1).

REFERENCES

Braatz, J. A., Wilson, A. S., Henkel, C., Gough, R., & Sinclair, M. 2003, ApJS, 146, 249

Braine, J., Guelin, M., Dumke, M., Brouillet, N., Herpin, F., & Wielebinski, R. 1997, A&A, 326, 963

Cecil, G., Bland-Hawthorn, J., & Veilleux, S. 2002, ApJ, 576, 745

Cecil, G., Bland-Hawthorn, J., Veilleux, S., & Filippenko, A. V. 2001, ApJ, 555, 338

Claussen, M. J., Diamond, P. J., Braatz, J. A., Wilson, A. S., & Henkel, C. 1998, ApJ, 500, L129

Cotton, W. D., Condon, J. J., & Arbizzani, E. 1999, ApJS, 125, 409

Deguchi, S. 1977, PASJ, 29, 669

Dunne, L., Eales, S., Edmunds, M., Ivison, R., Alexander, P., & Clements, D. L. 2000, MNRAS, 315, 115

Duric, N. & Seaquist, E. R. 1988, ApJ, 326, 574

Elitzur, M., Hollenbach, D. J., & McKee, C. F. 1989, ApJ, 346, 983

Feldman, P. A., Matthews, H. E., Cunningham, C. T., Hayward, R. H., Wade, J. D., Amano, T., & Scappini, F. 1991, JRASC, 85, 191

Gallimore, J. F., Baum, S. A., O'Dea, C. P., Brinks, E., & Pedlar, A. 1996, ApJ, 462, 740

Greenhill, L. 2002, in IAU Symposium, 381

Greenhill, L. J., et al. 2003, ApJ, 590, 162

Greenhill, L. J., Henkel, C., Becker, R., Wilson, T. L., & Wouterloot, J. G. A. 1995a, A&A, 304, 21

Greenhill, L. J., Jiang, D. R., Moran, J. M., Reid, M. J., Lo, K. Y., & Claussen, M. J. 1995b, ApJ, 440, 619

Hagiwara, Y., Henkel, C., Sherwood, W. A., & Baan, W. A. 2002, A&A, 387, L29

Hagiwara, Y., Klöckner, H.-R., & Baan, W. A. 2004, MNRAS, 353, 1055

Heckman, T. M. 1980, A&A, 87, 152

Hildebrand, R. H. 1983, QJRAS, 24, 267

Ho, L. C., Filippenko, A. V., & Sargent, W. L. W. 1997, ApJS, 112, 315

Jaffe, W., et al. 2004, Nature, 429, 47

Kartje, J. F., Königl, A., & Elitzur, M. 1999, ApJ, 513, 180

Koda, J., Sofue, Y., Kohno, K., Nakanishi, H., Onodera, S., Okumura, S. K., & Irwin, J. A. 2002, ApJ, 573, 105

Kondratko, P. T., Greenhill, L. J., & Moran, J. M. 2005, ApJ, 618, 618

Maloney, P. R. 2002, PASA, 19, 401

Melnick, G. J., Menten, K. M., Phillips, T. G., & Hunter, T. 1993, ApJ, 416, L37

Menten, K. M. & Melnick, G. J. 1989, ApJ, 341, L91

—. 1991, ApJ, 377, 647

Menten, K. M., Melnick, G. J., & Phillips, T. G. 1990a, ApJ, 350, L41

Menten, K. M., Melnick, G. J., Phillips, T. G., & Neufeld, D. A. 1990b, ApJ, 363, L27

Middelberg, E., et al. 2004, A&A, 417, 925

Miyoshi, M., Moran, J., Herrnstein, J., Greenhill, L., Nakai, N., Diamond, P., & Inoue, M. 1995, Nature, 373, 127

Neufeld, D. A., Maloney, P. R., & Conger, S. 1994, ApJ, 436, L127

Neufeld, D. A. & Melnick, G. J. 1991, ApJ, 368, 215

Peck, A. B., Henkel, C., Ulvestad, J. S., Brunthaler, A., Falcke, H., Elitzur, M., Menten, K. M., & Gallimore, J. F. 2003, ApJ, 590, 149

Phillips, T. G., Kwan, J., & Huggins, P. J. 1980, in IAU Symp. 87: Interstellar Molecules, 21–24

Prieto, M. A., et al. 2004, ApJ, 614, 135

Sawada-Satoh, S., Inoue, M., Shibata, K. M., Kameno, S., Migenes, V., Nakai, N., & Diamond, P. J. 2000, PASJ, 52, 421

Scoville, N. 1993, Mir Cookbook

Sofue, Y. 1999, Advances in Space Research, 23, 949

Trotter, A. S., Greenhill, L. J., Moran, J. M., Reid, M. J., Irwin, J. A., & Lo, K. 1998, ApJ, 495, 740

Waters, J. W., et al. 1980, ApJ, 235, 57

Yamauchi, A., Nakai, N., Sato, N., & Diamond, P. 2004, PASJ, 56, 605

Yates, J. A., Field, D., & Gray, M. D. 1997, MNRAS, 285, 303

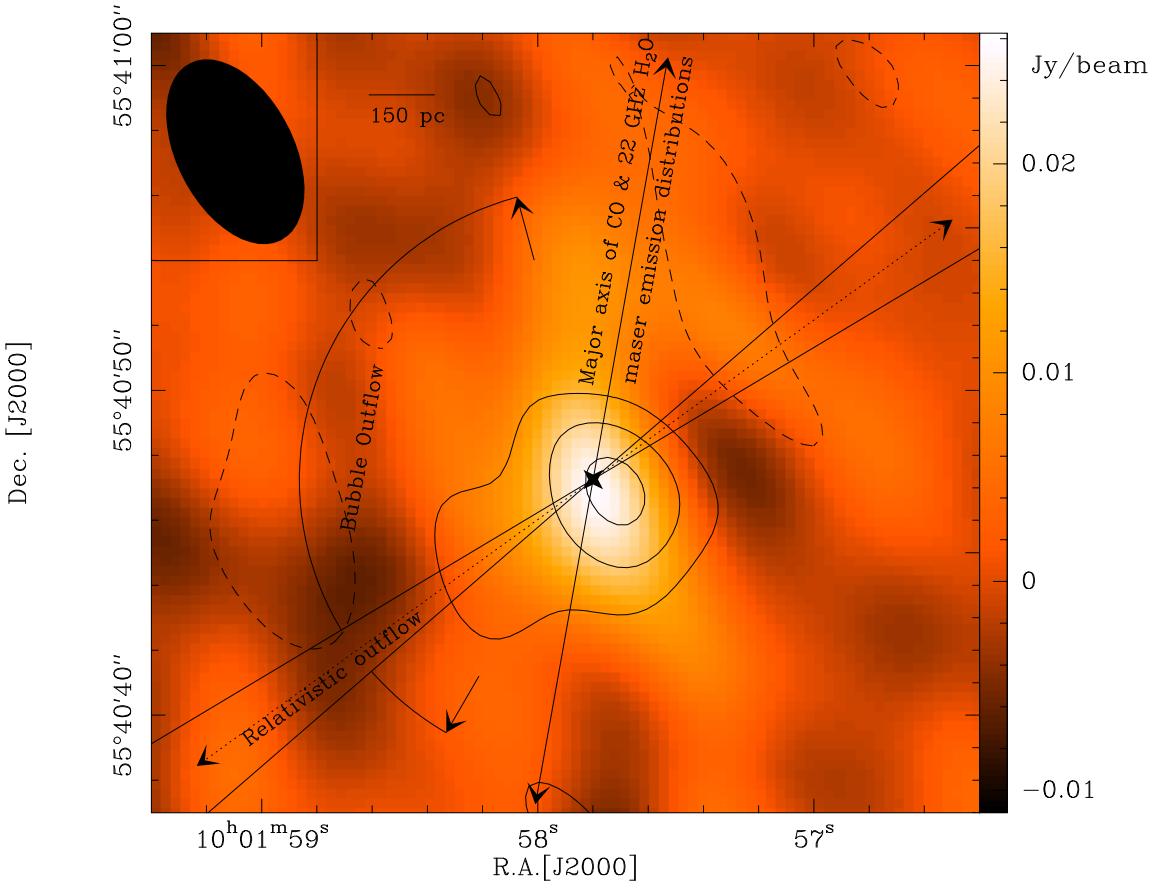

Fig. 1.— *(filled color contours)* Millimeter continuum image of NGC 3079 at 193 GHz observed with the SMA. Peak flux density is 27 mJy bm^{-1} with a 1σ r.m.s. of 2.5 mJy bm^{-1}; integrated continuum flux density is 53 mJy. *(line contours)* 183 GHz maser emission at 1017 km s^{-1} (optical, heliocentric). Peak maser flux density in the image is 0.39 Jy bm^{-1}. Positive emission is shown in solid lines and negative features in dashed contours. Contours are $k \times 2\sigma$, where $k = -1, 1, 2, 3$ and 1σ=56 mJy bm^{-1}. The black cross marks the position of peak 22 GHz H_2O maser emission at 956 km s^{-1}: $\alpha_{2000} = 10^h01^m57^s.802 \pm 0.001$, $\delta_{2000} = 55^o40'47''.26 \pm 0.01$ (Kondratko et al. 2005). The black solid arrow indicates the P.A. (∼-10° east of north) of the pc-scale 22 GHz H_2O maser disk (Kondratko et al. 2005) and of the kpc-scale CO disk (Koda et al. 2002). The dashed arrow marks the direction of relativistic outflow with uncertainty depicted by bracketing solid lines of P.A. 126° ± 5° (Trotter et al. 1998; Sawada-Satoh et al. 2000; Middelberg et al. 2004; Kondratko et al. 2005). The arc to the east denotes the opening angle of the kpc-scale superbubble outflowing from the galactic nucleus (e.g., Cecil et al. 2002). The SMA synthesized beam has FWHM of 5.″9 x 3.″4 (upper sideband) and 6.″1 x 3.″6 (lower sideband, shown top left), with a P.A. of 27° in both cases.

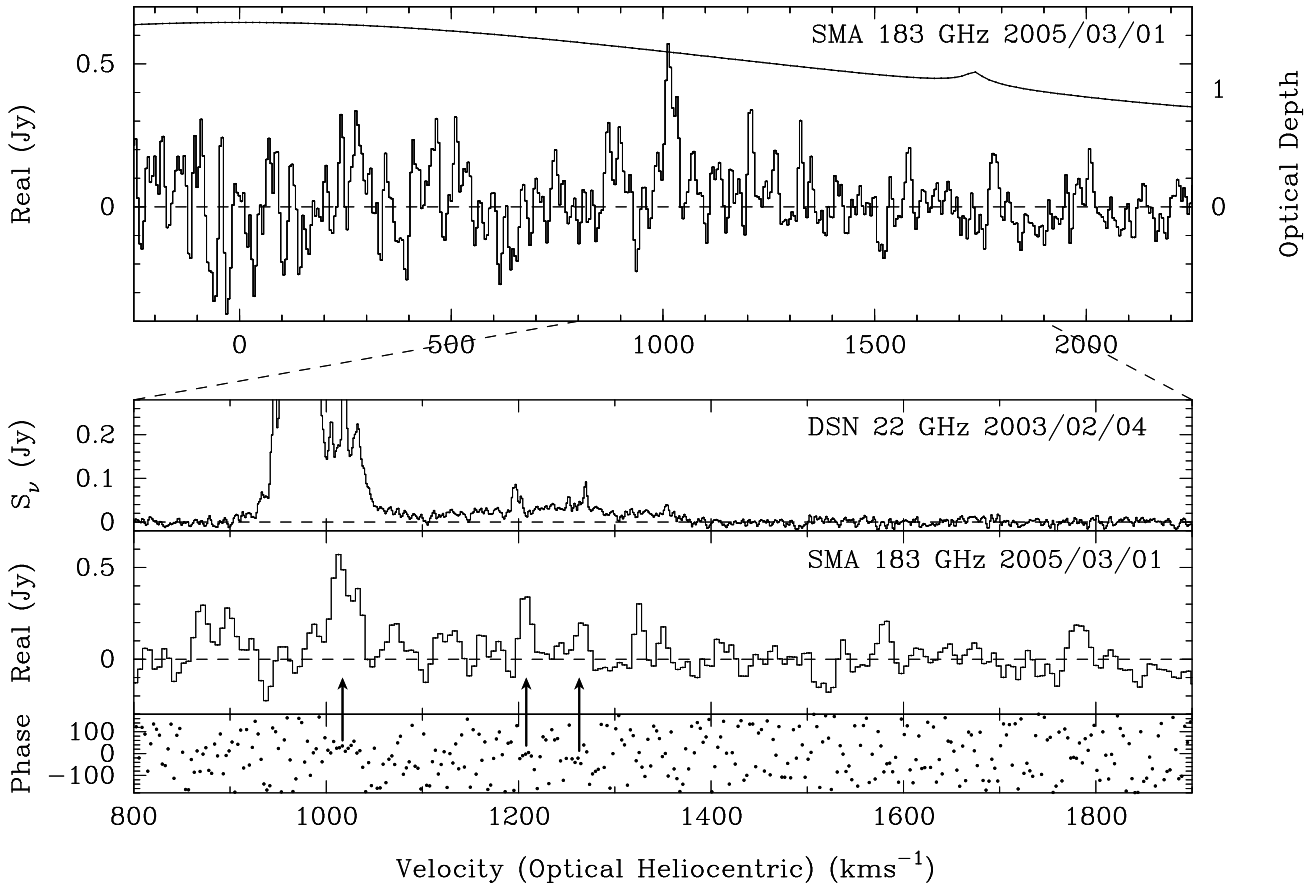

Fig. 2.— 183 GHz maser spectrum towards the nucleus of NGC 3079 corrected for atmospheric absorption obtained with the SMA. *(top panel)* Real part of the spectrum exhibiting a ∼0.55 Jy feature at a velocity of 1017 km s^{-1}. The channel spacing is 5 km s^{-1}. Atmospheric opacity for a zenith angle of 50^{o} is shown by the dotted line; peaks at 1850 and 2150 km s^{-1} are due to ozone. Note that the noise rises at lower velocities due to the effect of atmospheric absorption. *(upper bottom panel)* 22 GHz spectrum obtained with a DSN 70 m antenna (Kondratko, private communication) between 800 – 1900 km s^{-1}. *(middle bottom)* Real part of the 183 GHz SMA spectrum between 800 – 1900 km s^{-1}. *(lower bottom)* Corresponding fringe phase. Tentative maser features at 1208 and 1265 km s^{-1} are also noted with arrows.

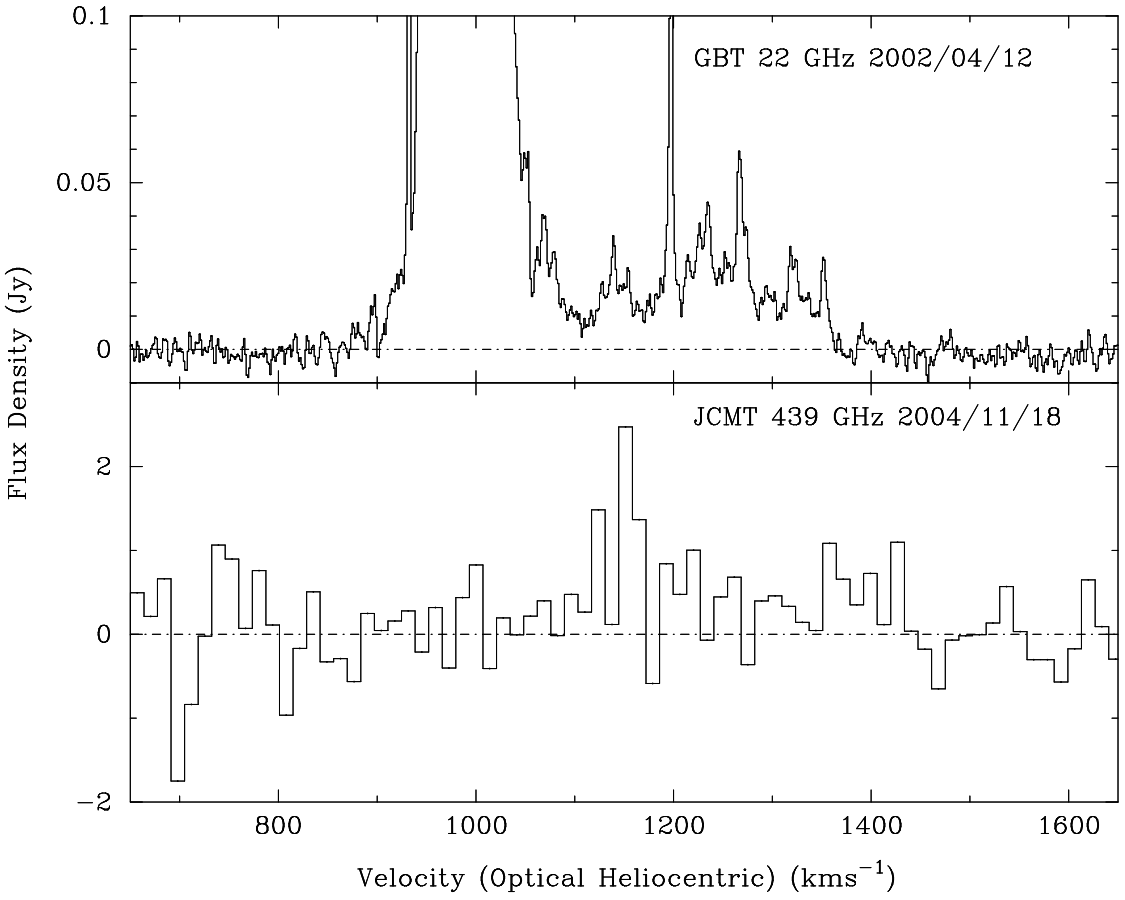

Fig. 3.— *(top)* 22 GHz spectrum obtained using the GBT from Braatz et al. (2003). *(bottom)* 439 GHz H_2O emission towards NGC 3079 observed with the JCMT. Peak flux density is 2.5 Jy, and the 1σ r.m.s. is 0.5 Jy. The channel spacing is 13.7 km s^{-1}.